Thai Journal of **Math**ematics
Volume 19 Number 3 (2021)
Pages 971–980

http://thaijmath.in.cmu.ac.th

ISSN 1686-0209

Development of a Genetically Integrated PBPK Model for Predicting Uric Acid Homeostasis in Humans

Noppavit Kaewlin[1,2], **Monrudee Liangruksa**[3,*] **and Teeraphan Laomettachit**[1,4,*]

[1] *Bioinformatics and Systems Biology Program, School of Bioresources and Technology, King Mongkut's University of Technology Thonburi (KMUTT), Bangkok, Thailand*
e-mail : por_noppavit@hotmail.com (N. Kaewlin); teeraphan.lao@kmutt.ac.th (T. Laomettachit)

[2] *School of Information Technology, King Mongkut's University of Technology Thonburi (KMUTT), Bangkok, Thailand*

[3] *National Nanotechnology Center (NANOTEC), National Science and Technology Development Agency (NSTDA), Pathum Thani 12120, Thailand*
e-mail : monrudee@nanotec.or.th (M. Liangruksa)

[4] *Theoretical and Computational Physics (TCP) Group, Center of Excellence in Theoretical and Computational Science (TaCS-CoE), King Mongkut's University of Technology Thonburi (KMUTT), Bangkok, Thailand*

Abstract Serum uric acid (SUA) balance is mainly regulated by the excretion and reabsorption by the kidneys. Much attention has recently been focused on the genetic variation of renal uric acid transporter genes that affect uric acid homeostasis. Here, we have developed a system of equations to study the human uric acid homeostasis using the physiologically based pharmacokinetic (PBPK) model. The PBPK model incorporates blood flow and tissue compartment of organs to describe how uric acid is distributed within the body. We have also implemented the concept of sub-compartments within the kidneys that allows the model to integrate the genetics of individual patients. We chose to model patients with single nucleotide polymorphisms (SNPs) on the *SLC2A9* gene (encoding the urate transporter protein, GLUT9) because the gene variation directly affects the amount of uric acid excreted and reabsorbed by the kidneys. SUA levels predicted from our model simulations of the wild-type and several variants of GLUT9 show good agreement with the experimental observations. Our model development results in a framework for implementing genetic factors as a subsystem of PBPK modeling while giving way to a better representation of human physiology in a highly complex system.

MSC: 37N25; 92-10
Keywords: physiologically based pharmacokinetic modeling; single nucleotide polymorphism; uric acid homeostasis

Submission date: 27.04.2021 / Acceptance date: 20.07.2021

Published by The Mathematical Association of Thailand.

1. Introduction

Body uric acid homeostasis is maintained by a balance between the production in the liver and renal/intestinal excretion [1]. Long-term excess uric acid in the blood (hyperuricemia) can lead to the formation of uric crystals in tissues and joints, causing an inflammatory response and pain [2]. A too lower amount of uric acid due to increased uric acid clearance causes hypouricemia, a relatively rare condition compared to its counterpart. Hypouricemia has been linked to nephrolithiasis and exercise-induced acute renal failure [3].

Several transmembrane proteins have been reported to be involved with the kidney's dysfunction, which leads to unbalanced serum uric acid (SUA) levels. For example, GLUT9, ABCG2, and URAT1 are the three core proteins among others in the maintenance of the SUA level [4, 5]. Glucose transporter 9 (GLUT9), a high-affinity glucose transporter encoded by the gene *SLC2A9*, reabsorbs uric acid within the kidneys and transports it back to the blood. Single nucleotide polymorphisms (SNPs) of the *SLC2A9* gene were identified to correspond to hypouricemia cases [6]. The ATP-binding cassette transporter ABCG2 is responsible for the excretion of uric acid. Several SNPs in the *ABCG2* gene are associated with hyperuricemia and gout [7]. Urate transporter 1 (URAT1), encoded by the *SLC22A12* gene, is a target of both uricosuric and antiuricosuric agents. A previous study has identified several *SLC22A12* SNPs that can potentially cause hyperuricemia [8].

The dynamics of uric acid levels in the body can be studied *in silico* by physiologically based pharmacokinetic (PBPK) modeling. This type of model is based on human physiology, considering important organs and tissues as individual compartments interconnected via the blood [9]. Compartmental models have been used to study the SUA level in the human body before [10, 11]. However, to the best of our knowledge, no study aims to integrate genetic factors into the PBPK modeling of uric acid. Therefore, there is a need for a model of the kidneys and other compartments to take into account the genes that affect uric acid regulation.

This work aims to construct a mathematical model that describes the distribution of uric acid among different compartments of the human body using mass-balance equations. We utilize perfusion rate-limited PBPK modeling and extend it to integrate genetic variants of GLUT9 by translating the genetic information into appropriate kinetic rates of uric acid reabsorption in the kidneys. The present work only focuses on the genetic information of GLUT9 due to the availability of the data. Model simulations predict the SUA levels, which are in good agreement with experimental observations from patients with various genetic polymorphisms. The model will allow for an in-depth look at the homeostasis of uric acid in the body, which will enable us to develop better methods for controlling SUA levels.

2. Model Development

Figure 1 depicts compartments and sub-compartments of the human body involved in the regulation and distribution of uric acid with the arrows representing mass transport of uric acid from one compartment to another. The diagram is translated into Eq. 2.1–2.9 to describe production, transportation, and excretion rates of uric acid.

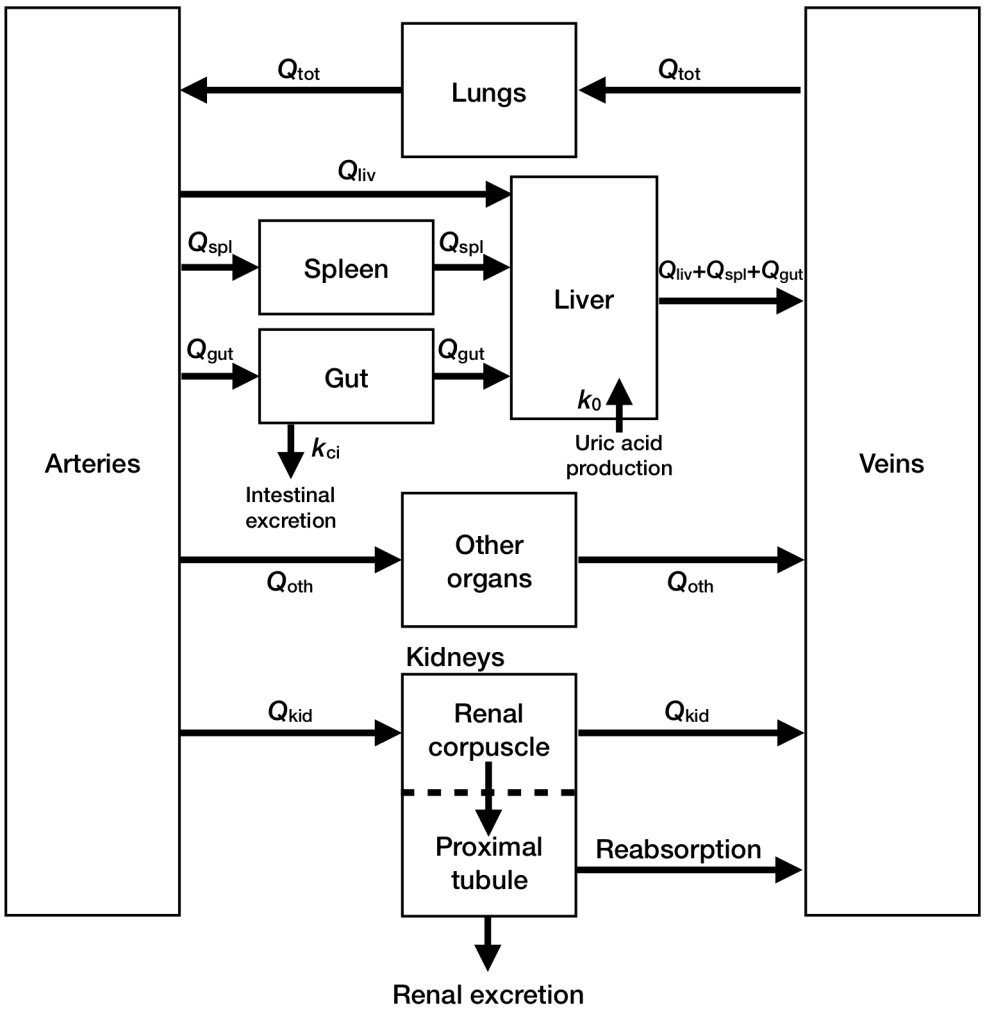

FIGURE 1. **Model compartments and mass transport among compartments.** Boxes represent compartments in the human body involved in the regulation and distribution of uric acid. Arrows represent mass transport of uric acid to and from the compartments, with Q's denoting the blood flow rates (L/h). (See Table 1 for a full list of model parameters and definitions.) Uric acid is produced in the liver and excreted from the body via the intestine (gut) and the kidneys.

$$\frac{\mathrm{d}A_{\mathrm{lun}}}{\mathrm{d}t} = Q_{\mathrm{tot}} \cdot \left(\frac{A_{\mathrm{v}}}{V_{\mathrm{v}}} - \frac{A_{\mathrm{lun}}}{V_{\mathrm{lun}} \cdot P_{\mathrm{lun}}}\right), \tag{2.1}$$

$$\frac{\mathrm{d}A_{\mathrm{a}}}{\mathrm{d}t} = Q_{\mathrm{tot}} \cdot \left(\frac{A_{\mathrm{lun}}}{V_{\mathrm{lun}} \cdot P_{\mathrm{lun}}} - \frac{A_{\mathrm{a}}}{V_{\mathrm{a}}}\right), \tag{2.2}$$

$$\frac{\mathrm{d}A_{\mathrm{gut}}}{\mathrm{d}t} = Q_{\mathrm{gut}} \cdot \left(\frac{A_{\mathrm{a}}}{V_{\mathrm{a}}} - \frac{A_{\mathrm{gut}}}{V_{\mathrm{gut}} \cdot P_{\mathrm{gut}}}\right) - k_{\mathrm{ci}} \cdot \frac{A_{\mathrm{gut}}}{V_{\mathrm{gut}}}, \tag{2.3}$$

$$\frac{\mathrm{d}A_{\mathrm{spl}}}{\mathrm{d}t} = Q_{\mathrm{spl}} \cdot \left(\frac{A_{\mathrm{a}}}{V_{\mathrm{a}}} - \frac{A_{\mathrm{spl}}}{V_{\mathrm{spl}} \cdot P_{\mathrm{spl}}}\right), \tag{2.4}$$

$$\begin{aligned}\frac{\mathrm{d}A_{\mathrm{liv}}}{\mathrm{d}t} &= k_0 + Q_{\mathrm{liv}} \cdot \left(\frac{A_{\mathrm{a}}}{V_{\mathrm{a}}} - \frac{A_{\mathrm{liv}}}{V_{\mathrm{liv}} \cdot P_{\mathrm{liv}}}\right) + Q_{\mathrm{gut}} \cdot \left(\frac{A_{\mathrm{gut}}}{V_{\mathrm{gut}} \cdot P_{\mathrm{gut}}} - \frac{A_{\mathrm{liv}}}{V_{\mathrm{liv}} \cdot P_{\mathrm{liv}}}\right) \\ &\quad + Q_{\mathrm{spl}} \cdot \left(\frac{A_{\mathrm{spl}}}{V_{\mathrm{spl}} \cdot P_{\mathrm{spl}}} - \frac{A_{\mathrm{liv}}}{V_{\mathrm{liv}} \cdot P_{\mathrm{liv}}}\right),\end{aligned} \tag{2.5}$$

$$\frac{\mathrm{d}A_{\mathrm{corp}}}{\mathrm{d}t} = Q_{\mathrm{kid}} \cdot \left(\frac{A_{\mathrm{a}}}{V_{\mathrm{a}}} - \frac{A_{\mathrm{corp}}}{V_{\mathrm{corp}} \cdot P_{\mathrm{kid}}}\right) - GFR \cdot \frac{A_{\mathrm{corp}}}{V_{\mathrm{corp}}}, \tag{2.6}$$

$$\frac{\mathrm{d}A_{\mathrm{prox}}}{\mathrm{d}t} = GFR \cdot \left(\frac{A_{\mathrm{corp}}}{V_{\mathrm{corp}}} - \frac{A_{\mathrm{prox}}}{V_{\mathrm{prox}}}\right) - \sigma \cdot V_{\max} \cdot \frac{\frac{A_{\mathrm{prox}}}{V_{\mathrm{prox}}}}{K_{\mathrm{m}} + \frac{A_{\mathrm{prox}}}{V_{\mathrm{prox}}}}, \tag{2.7}$$

$$\frac{\mathrm{d}A_{\mathrm{oth}}}{\mathrm{d}t} = Q_{\mathrm{oth}} \cdot \left(\frac{A_{\mathrm{a}}}{V_{\mathrm{a}}} - \frac{A_{\mathrm{oth}}}{V_{\mathrm{oth}} \cdot P_{\mathrm{oth}}}\right), \tag{2.8}$$

$$\begin{aligned}\frac{\mathrm{d}A_{\mathrm{v}}}{\mathrm{d}t} &= (Q_{\mathrm{liv}} + Q_{\mathrm{gut}} + Q_{\mathrm{spl}}) \cdot \frac{A_{\mathrm{liv}}}{V_{\mathrm{liv}} \cdot P_{\mathrm{liv}}} + Q_{\mathrm{kid}} \cdot \frac{A_{\mathrm{corp}}}{V_{\mathrm{corp}} \cdot P_{\mathrm{kid}}} \\ &\quad + Q_{\mathrm{oth}} \cdot \frac{A_{\mathrm{oth}}}{V_{\mathrm{oth}} \cdot P_{\mathrm{oth}}} - Q_{\mathrm{tot}} \cdot \frac{A_{\mathrm{v}}}{V_{\mathrm{v}}} + \sigma \cdot V_{\max} \cdot \frac{\frac{A_{\mathrm{prox}}}{V_{\mathrm{prox}}}}{K_{\mathrm{m}} + \frac{A_{\mathrm{prox}}}{V_{\mathrm{prox}}}}.\end{aligned} \tag{2.9}$$

In the equations, A's denote the amount of uric acid (μmol) in tissue compartments, Q's the blood flow rate (L/h), V's the volume of the compartments, P's the partition coefficients of uric acid between tissue and its blood. The subscripts lun, a, gut, spl, liv, corp, prox, oth, and v denote lungs, arteries, gut, spleen, liver, renal corpuscles, proximal tubules, other organs, and veins, respectively. Q_{tot} is the total blood flow rate (L/h). A full list of model parameters and definitions can be found in Table 1. Note that the physiological parameter values (Q's and V's) in Table 1 are from an average person with a weight of 73 kg.

Uric acid is produced in the liver as a consequence of purine breakdown due to the activity of xanthine oxidase [12]. In our model, uric acid is produced in the liver with the rate k_0 (Eq. 2.5). It is released into the venous blood (Eq. 2.9), and then transported to lungs (Eq. 2.1), and, subsequently, the arterial blood compartment (Eq. 2.2). Uric acid in the arterial blood is distributed into the gut (Eq. 2.3), spleen (Eq. 2.4), liver (Eq. 2.5), kidneys (Eq. 2.6 and 2.7), and the other organs (Eq. 2.8), before re-entering into the venous blood compartment. In the kidneys, uric acid first enters the renal corpuscle sub-compartment (Eq. 2.6) within the kidneys' cortex. The uric acid is then filtered into the proximal tubule sub-compartment with the rate GFR (Eq. 2.7). Within the proximal tubule sub-compartment, uric acid can be reabsorbed back to the venous blood compartment by uric acid transporter proteins, GLUT9, embedded in the proximal tubule cells. Uric acid that is not reabsorbed is excreted as urine. Uric acid is also excreted in

TABLE 1. **Model parameters**

Parameter	Value	Description	Reference
k_0	300 μmol/h	Uric acid production rate	[10]
GFR	7.8 L/h	Glomerular filtration rate	[11]
k_{ci}	0.3 L/h	Intestinal uric acid clearance rate	[11]
$V_{\max}$	$1.28 \times 10^{-2}\mu$mol/h	Maximum rate of urate reabsorption by wild-type GLUT9	[6]
K_{m}	433 μmol/L	Michaelis-Menten constant of wild-type GLUT9	[6]
σ	2×10^6	Scaling factor	fitting
Q_{tot}	390 L/h	Total blood flow rate	[15]
Q_{liv}	99.45 L/h	Liver's blood flow rate	[15]
Q_{gut}	58.5 L/h	Gut's blood flow rate	[15]
Q_{spl}	11.7 L/h	Spleen's blood flow rate	[15]
Q_{kid}	74.1 L/h	Kidneys' blood flow rate	[15]
Q_{oth}	146.25 L/h	Other organs' blood flow rate	[15]
V_{liv}	1.8 L	Liver's volume	[15]
V_{gut}	1.3 L	Gut's volume	[15]
V_{spl}	0.15 L	Spleen's volume	[15]
V_{corp}	9.45×10^{-2} L	Renal corpuscles' volume	[16, 17]
V_{prox}	9.45×10^{-2} L	Renal proximal tubules' volume	[16, 17]
V_{lun}	0.5 L	Lungs' volume	[15]
V_{v}	4.2 L	Venous blood volume	[15]
V_{a}	1.4 L	Arterial blood volume	[15]
V_{oth}	63.46 L	Other organs' volume	[15]
P_{liv}	1.02	Partition coefficient for liver	[10, 14]
P_{gut}	0.97	Partition coefficient for gut	[10, 14]
P_{spl}	1.07	Partition coefficient for spleen	[10, 14]
P_{kid}	1.06	Partition coefficient for kidneys	[10, 14]
P_{lun}	0.97	Partition coefficient for lungs	[10, 14]
P_{oth}	1.00	Partition coefficient for other organs	estimated

the intestine (gut) [13] with the rate k_{ci}. Since the unbound fraction of uric acid from plasma proteins is about 1.0 [10], the total fraction of uric acid in the circulation system is subject to excretion and reabsorption. Finally, the partition coefficient of each tissue is calculated based on the Poulin and Theil method [14], using physicochemical parameters of uric acid provided in [10].

In Eq. 2.7 and 2.9, we represent the reabsorption activity meditated by GLUT9 with the Michaelis-Menten kinetics, $\sigma \cdot V_{\max} \cdot \frac{A_{\text{prox}}}{V_{\text{prox}}}/(K_{\text{m}} + \frac{A_{\text{prox}}}{V_{\text{prox}}})$, where $V_{\max}$, K_{m}, and σ are the maximum velocity of uric acid transport by the GLUT9 protein, a Michaelis-Menten constant of the protein, and a scaling factor, respectively. In a study by Ruiz, et al. (2018) [6], different genetic variants of the GLUT9 proteins were expressed on the cell membrane of *Xenopus laevis* oocytes. The authors then incubated the oocytes with uric acid, and the two-electrode voltage clamp was used to measure the current that passed through the protein channels. The experiment yielded the values of $V_{\max}$ and K_{m} for each GLUT9 variant as shown in Table 2. Therefore, the genetic variants can be incorporated into the model by modifying the constants $V_{\max}$ and K_{m} accordingly. The scaling factor σ is added to the Michaelis-Menten kinetics in Eq. 2.7 and 2.9 to scale the activity of

GLUT9 measured in the oocytes to the activity of the proteins expressed in the human kidneys. The scaling factor is usually estimated by *in vitro-in vivo* extrapolation (IVIVE). However, information regarding the amount of GLUT9 expressed in the oocytes compared to the total number of the proteins expressed in the whole human kidneys is not available from the experiments. Thus instead, we estimated the scaling factor by fitting our model prediction of the wild-type SUA to the experiment. As all GLUT9 variants studied in the present work were expressed at a comparable level compared to the wild-type in the oocyte experiment [6], the wild-type and the variants take the same value of the scaling factor.

As the values of $V_{\max}$ in [6] were reported in μA (μcoulomb/s), we can divide them by the Faraday constant to find the amount of uric acid per time unit (μmol/h), a calculation commonly used in electrolysis. The conversion is shown in Eq. 2.10.

$$V_{\max} = \frac{\phi \cdot V_{\max}^{\exp}}{F}, \tag{2.10}$$

where $V_{\max}$ is the maximum velocity of uric acid transport by the protein used in our model (μmol/h), $V_{\max}^{\exp}$ is the maximum velocity of uric acid transport by the protein measured experimentally in [6] (μA), F is the Faraday constant = 96,485 μcoulomb/μmol electrons, and ϕ=3600 is a factor to convert second to hour. The converted values of $V_{\max}$ are shown in Table 2.

TABLE 2. **GLUT9 parameters**

Genetic variant	$V_{\max}^{\exp}$ (μA) [6]	$V_{\max}$ (μmol/h)	K_{m} (μmol/L) [6]
Wild-type (WT)	0.347	1.2839×10^{-2}	433
R171C	0.345	1.2765×10^{-2}	411
R198C	0.181	0.6697×10^{-2}	603
N333S	0.260	0.962×10^{-2}	1221
R380W	0.076	0.2812×10^{-2}	839
P412R	0.313	1.1581×10^{-2}	434

3. Results and Discussion

We solve numerically Eq. 2.1– 2.9 with parameter values in Table 1 using XPPAUT (http://www.math.pitt.edu/~bard/xpp/xpp.html) to obtain time-series dynamics of the uric acid levels in different compartments. Fig. 2 shows the simulated steady-state uric acid levels of a healthy person with a weight of 73 kg with a normal activity of GLUT9 ($V_{\max}$=$1.2839\times10^{-2}$$\mu$mol/h and K_{m}=433 μmol/L [6]). The simulation shows the concentration of the SUA (uric acid in the venous blood compartment) at approximately 250 μmol/L (4.2 mg/dL), which is in a normal range. The uric acid level in the kidneys is lowest as the compartment is the main site for uric excretion.

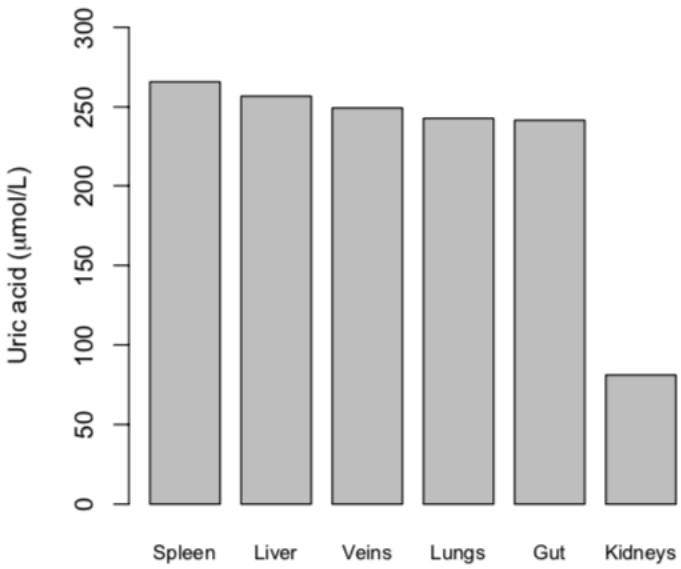

FIGURE 2. **Uric acid distribution in the human body.** The simulated distribution of the uric acid levels in a healthy person with a weight of 73 kg with a normal activity of GLUT9 (V_{max}=1.2839×10^{-2} μmol/h and K_m=433 μmol/L [6]).

Figure 3 compares the steady-state SUA levels in patients with different genetic variations between model simulations and experimental data [6]. The simulations are performed by using the values of V_{max} and K_m in Table 2. The results show that simulations from our model, which take into account the genetic variations that affect the reabsorption rates of the proteins in the kidneys, are in good agreement with experiments for the wild-type (WT) and three other SNPs (R171C, R198C, and R380W). For the other two SNPs (P412R and N333S), our model predicts higher SUA levels than those observed in the patients.

The patient carrying the genetic variant P412R suffered from hypouricemia, having a SUA level of 143 μmol/L (2.4 mg/dL) [18]. However, the V_{max} and K_m of the variant measured by the oocyte experiment in [6] were similar to those of the wild-type (Table 2), which is why our model simulation of the genetic variant yields a SUA of 232 μmol/L (3.9 mg/dL). However, another study [18] reported differently that the variant P412R exhibited a significantly decreased urate transport activity compared to the wild-type. Therefore, this discrepancy between the experiments needs to be reconciled before the urate transport activity of the variant can be incorporated accurately into the model.

The genetic variant N333S was reported to be genetically associated with another SNP (G216R) [19]. Since the V_{max} and K_m of G216R were not reported, our simulation for the patient with N333S variant could not account for the associated SNP at G216R, which may explain the discrepancy between the SUA level from our simulation and the observation.

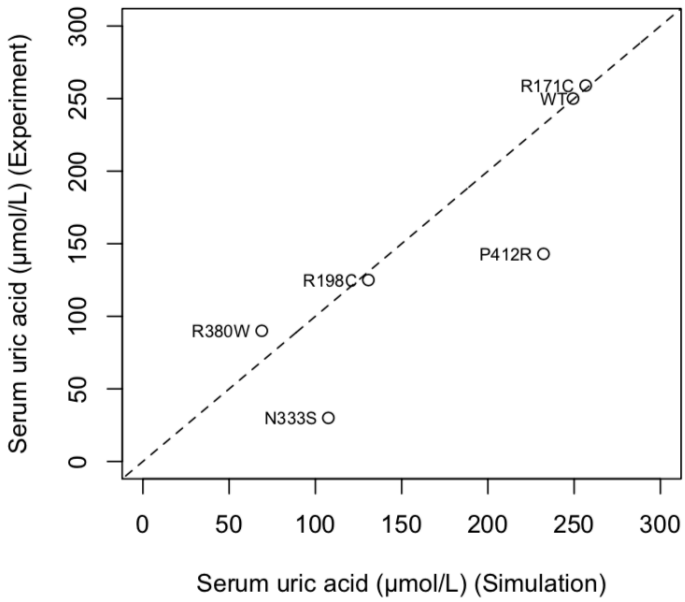

FIGURE 3. **Simulations of patients with genetic variants.** The serum uric acid (SUA) levels are compared between model predictions (simulation) and observations (experiment) [6] from patients with genetic variation in *SLC2A9* (encoding GLUT9).

4. CONCLUSION

We have developed a system of equations to study human uric acid homeostasis using the physiologically based pharmacokinetic (PBPK) model. We have also implemented the concept of sub-compartments within the kidneys that allows the model to incorporate the genetic information of individual patients. We focused on the polymorphisms of the *SLC2A9* gene whose mutations are mostly loss-of-function [6], causing hypouricemia. Our model, which integrates genetic variations that affect the kidneys' function, simulates the SUA levels that are in good agreement with the observations in the patients.

During the development of this work, the amount of data that we can obtain about the urate transporter proteins in question is highly limited. As such, we hope that in the future, we can expand our model to incorporate more transmembrane proteins that regulate uric acid homeostasis by the integration of their genetics. By modeling the contribution of these proteins to the SUA level, the model predictions may lead to better therapeutic approaches and may enable us to make personalized medical interventions for individual patients with hyper/hypouricemia.

Acknowledgements

T.L. and M.L. gratefully acknowledge the financial support from the Asahi Glass Foundation. The authors are grateful to the editor and a reviewer for providing valuable suggestions and comments for this work.

References

[1] J. Maiuolo, F. Oppedisano, S. Gratteri, C. Muscoli, V. Mollace, Regulation of uric acid metabolism and excretion, International journal of cardiology 213 (2016) 8–14.

[2] M. Underwood, Diagnosis and management of gout, BMJ 332.7553 (2006) 1315–1319.

[3] Ch.M.M. Erley, R.R. Hirschberg, W. Hoefer, K. Schaefer, Acute renal failure due to uric acid nephropathy in a patient with renal hypouricemia, Klinische Wochenschrift 67 (5) (1989) 308–312.

[4] L. Xu, Y. Shi, S. Zhuang, N. Liu, Recent advances on uric acid transporters, Oncotarget 8.59 (2017) 100852.

[5] S.K. Nigam, V. Bhatnagar, The systems biology of uric acid transporters: the role of remote sensing and signaling, Current opinion in nephrology and hypertension 27 (4) (2018) 305.

[6] A. Ruiz, I. Gautschi, L. Schild, O. Bonny, Human mutations in SLC2A9 (Glut9) affect transport capacity for urate, Frontiers in physiology 9 (2018) 476.

[7] K.H. Yu, P.Y. Chang, S.C. Chang, Y.H. Wu-Chou, L.A. Wu, D.P. Chen, F.S. Lo, J.J. Lu, A comprehensive analysis of the association of common variants of *ABCG2* with gout, Scientific reports 7 (1) (2017) 1–8.

[8] S.K. Cho, S. Kim, J.Y. Chung, S.H. Jee, Discovery of URAT1 SNPs and association between serum uric acid levels and URAT1, BMJ open 5 (11) (2015).

[9] J.L. Campbell, R.A. Clewell, P.R. Gentry, M.E. Andersen, H.J. Clewell, Physiologically based pharmacokinetic/toxicokinetic modeling, Computational toxicology, Humana Press; Totowa, New Jersey, (2012), 439–499.

[10] M. Krauss, S. Schaller, S. Borchers, R. Findeisen, J. Lippert, L. Kuepfer, Integrating cellular metabolism into a multiscale whole-body model, PLOS computational biology 8 (10) (2012) e1002750.

[11] S. Aksenov, C.C. Peck, U.G. Eriksson, D.R. Stanski, Individualized treatment strategies for hyperuricemia informed by a semi-mechanistic exposure-response model of uric acid dynamics, Physiological reports 6 (5) (2018) e13614.

[12] R.W. Watts, Symposium on gout and other disorders of purine metabolism: Uric acid production with particular reference to the role of xanthine oxidase and its inhibition, (1966), 287–292.

[13] A. Hosomi, T. Nakanishi, T. Fujita, I. Tamai, Extra-renal elimination of uric acid via intestinal efflux transporter BCRP/ABCG2, PLOS ONE 7 (2) (2012) e30456.

[14] P. Poulin, F.P. Theil, Prediction of pharmacokinetics prior to *in vivo* studies. 1. Mechanism-based prediction of volume of distribution, Journal of pharmaceutical sciences, 91 (1) (2002) 129–156.

[15] J. Valentin, Basic anatomical and physiological data for use in radiological protection: reference values: ICRP Publication 89, Annals of the ICRP 32 (3–4) (2002) 1–277.

[16] L. Garcia-Covarrubias, DR. Valdez, LA. Bermudez, R. Cordoba, F.J. Avelar, R.M. Villanueva, D. Ortuno, J.C. Hernandez, A. Garcia, I. Castro, Correlation of the renal cortex volume with the glomerular filtration rate in live donors for renal transplantation, Transplantation proceedings, 50 (2) (2018) 428–432.

[17] K. Wilhelm, K. Brigitte, Structural organization of the mammalian kidney, Seldin and Giebisch's The Kidney, Elsevier, 2008.

[18] N. Anzai, K. Ichida, P. Jutabha, T. Kimura, E. Babu, C.J. Jin, S. Srivastava, K. Kitamura, I. Hisatome, H. Endou, H. Sakurai, Plasma urate level is directly regulated by a voltage-driven urate efflux transporter URATv1 (SLC2A9) in humans, Journal of biological chemistry 283 (40) (2008) 26834–26838.

[19] B. Stiburkova, J. Taylor, A.M. Marinaki, I. Sebesta, Acute kidney injury in two children caused by renal hypouricaemia type 2, Pediatric nephrology 27 (8) (2012) 1411–1415.